Journal of Applied Electrochemistry **31**: 421–428, 2001.

Chlorate transport through ion-exchange membranes

S.A. PERUSICH* and S.M. REDDY
*Auburn University, Department of Chemical Engineering, 240 Ross Hall, Auburn, Alabama 36849-5127, USA (*author for correspondence)*

Received 8 March 2000; accepted in revised form 11 September 2000

Key words: chlor-alkali, equivzalent weight, membrane, perfluorocarbon, Nafion®, sodium chlorate

Abstract

A laboratory scale chlor-alkali membrane cell was used to measure the chlorate concentration in the outlet NaOH as a function of current density, temperature, film thickness, brine strength and various membrane properties. The chlorate concentration in the NaOH increased with increasing anolyte chlorate spiking level and temperature and decreasing current density and carboxylate film thickness and was strongly dependent on the type of ion-exchange membrane used. In addition, the presence or absence of sacrificial fibers in the membrane did not measurably influence the resultant chlorate concentration. Chlorate ions were transported to the catholyte side by diffusion and electroosmotic convection and transported toward the anolyte side by migration. This balance between the three modes of transport dictates the chlorate concentration present in the NaOH product.

1. Introduction

The transport of anions through a cation-exchange membrane is the subject of considerable fundamental and practical interest, and significant research has been done on understanding the production and ultimate contamination that these anions have on the desired product. One case that is of basic and applied interest but has not been studied in much detail is the chlorate ion transport in an electrochemical membrane cell.

Chlorate (ClO_3^-) can be formed in the anode or cathode compartments of a chlor-alkali membrane cell or in the membrane itself and eventually builds up in both the anolyte and catholyte streams. The 'impure' NaOH (NaOH containing high chlorate concentrations) cannot be used in certain applications. Specifically, high chlorate concentrations (i) cause corrosion of nickel process equipment, especially at $>50\%$ NaOH, (ii) give colour to epoxy resins, (iii) pose contamination problems in rayon manufacture, and (iv) lower yields in certain reactions (e.g., glutamic acid synthesis) [1–3]. It is desirable to reduce the chlorate concentration in the NaOH (catholyte) stream to a minimal acceptable value of about 10 ppm. The present paper presents experimental chlorate studies carried out in a laboratory size chlor-alkali electrochemical cell. A paper in preparation [4] will detail a theoretical model for the anion formation and transport.

In 1902, Foerster and Muller [5] did the first fundamental work to describe the mechanism of chlorate formation. Except under unusual conditions, their mechanism is still the accepted one and is described by the following five reactions:

$$\text{Anode:} \quad 2\,Cl^- \rightarrow Cl_2 + 2\,e^-$$

$$\text{Cathode:} \quad 2\,H_2O + 2\,e^- \rightarrow H_2 + 2\,OH^-$$

$$\text{Solution:} \quad Cl_2 + H_2O \rightleftharpoons Cl^- + H^+ + HOCl$$

$$HOCl \rightleftharpoons ClO^- + H^+$$

$$2\,HOCl + ClO^- \rightarrow ClO_3^- + 2\,Cl^- + H^+$$

A rough idea of the relative concentrations of sodium chlorate ($NaClO_3$) found in different chlor-alkali plants is given in Table 1. All NaOH concentrations are normalized to 50%. Since all new chlor-alkali plants use membrane technology and closed loop control with recycle loops is a desired goal for process control, the large concentration of chlorate in the NaOH product stream from membrane cells is of critical interest.

Chlorate in chlor-alkali cells has been investigated by a few research studies [6–10] which deal mainly with the chemistry of chlorate formation. A recent paper by Chen and Tilak [11] proposes a rough theoretical approach but does not account for the complex chlorate chemistry. In addition, several patents are available which seek to control chlorate by either adding a catalyst to the brine to prevent chlorate formation [12], purifying the recycled brine [13–20], or decomposing the chlorate in the exit NaOH stream well after the chlorate has been produced [21–24].

No studies exist that are known to the authors where the transport of chlorate through a membrane is

Table 1. Sodium chlorate concentrations found in industrial chlor-alkali plants

Plant	[NaOH]	[$NaClO_3$]
Diaphragm	50%	0.05–0.1%
Mercury	50%	1–5 ppm
Membrane (with recycle)	50%	10–70 ppm

hindered or eliminated by changing the membrane or polymer properties. If chlorate can be eliminated before it enters the catholyte chamber, costly purification of the NaOH stream can be avoided.

2. Experimental details

A chlor-alkali electrochemical membrane cell was used to evaluate the ion concentrations. The cell was built in-house and equipped with purified brine in a one pass (no recycle) anolyte system. Pure water was supplied to the cathode side. Samples of the two inlet and two outlet streams were taken for analysis. Typical lab cell parameters are listed in Table 2.

The membranes used for chlorate experiments were Nafion® (DuPont), Aciplex (Asahi Chemical), Flemion (Asahi Glass), and Dow Chemical's prototype membrane; all the chemical structures are given in Table 3, and the membranes are listed in Table 4. Membrane samples were analyzed by FTIR to determine the equivalent weight whenever possible and were completely converted to the Na^+ salt form before use in the cell [25]. Due to proprietary concerns, the Nafion® samples are listed anonymously, but sufficient detail about the membrane structure is given to analyse the resulting data. The nomenclature used in Table 4 for a membrane layer is given, for example, that '2-1050CR' means a 2 mil thick, 1050 g equiv^{-1} Nafion® CR (carboxylate) layer.

To accurately determine the chlorate concentration in caustic and brine, an analytical method based on the work of Stookey [26] was used. The technique uses ferrozine to react with Fe^{2+} (from ferrous ammonium sulfate) to form a magenta-coloured iron ligand. When chlorate is added to this solution, the Fe^{2+} reacts with the chlorate thus decreasing the ligand formation as well as the magenta colour. A colorimeter (Bran + Luebbe) was used to detect this change of colour which was then correlated to the chlorate composition. The calibration curve was generated by preparing chlorate standards in either water or 32% NaOH in the range of 1 to 12 ppm $NaClO_3$. All chlorate concentrations above the calibration range were diluted with either water or 32% NaOH prior to analysis.

Table 2. Laboratory cell parameters

Cell size	3″ diameter*
Brine strength	17–20 % wt
Brine feed	0.1–0.2 ml A^{-1} min^{-1}
Anode	DSA screen
Cathode	Nickel screen
Current density	1–5 kA m^{-2}
Electrode gap	Finite (3 mm)
Temp. range	80–90 °C
NaOH	32–33 % wt
$NaClO_3$ spiking	0–20 g l^{-1}

* 2″ diameter cell was used for Flemion experiments

Table 3. Polymer structures

Polymer	Chemical Structure
Nafion® sulfonate (XR)	$\sim CF_2–CF(–O–CF_2–CF(CF_3)–O–CF_2–CF_2–SO_3^-Na^+)–(CF_2–CF_2)_n\sim$
Nafion® carboxylate (CR)	$\sim CF_2–CF(–O–CF_2–CF(CF_3)–O–CF_2–CF_2–CO_2^-Na^+)–(CF_2–CF_2)_n\sim$
Flemion 'XR'	Same as Nafion® XR
Flemion 'CR'	$\sim CF_2–CF(–O–CF_2–CF_2–CF_2–CO_2^-Na^+)–(CF_2–CF_2)_n\sim$
Aciplex 'XR'	$\sim CF_2–CF(–O–CF_2–CF(CF_3)–O–CF_2–CF_2–(CF_2)_i–SO_3^-Na^+)–(CF_2–CF_2)_n\sim$
Aciplex 'CR'	Same as Nafion® CR
Dow 'XR'	$\sim CF_2–CF(–O–CF_2–CF_2–SO_3^-Na^+)–(CF_2–CF_2)_n\sim$
Dow 'CR'	$\sim CF_2–CF(–O–CF_2–CF_2–CO_2^-Na^+)–(CF_2–CF_2)_n\sim$

3. Discussion of experimental results

3.1. *Long term data*

Chlorate data taken from the NaOH outlet in unspiked cells are shown in Figure 1 for an array of ion-exchange membranes. All data (except those for the Dow membrane) range from 0.3 to 4.9 ppm $NaClO_3$, values which are well within the acceptable range (below 10 ppm). The range of data for any single membrane varies from 0.1 to 3.2 ppm, all run under similar operating conditions. The Dow membrane is the only exception yielding chlorate concentrations of 19 to 31 ppm. The presence or absence of sacrificial fibers in the membranes did not significantly affect the measured chlorate values. The error in the individual chlorate measurements is less than 0.1 ppm.

The data in Figure 1 simulate a cell running without a brine recirculation loop where the chlorate produced in the cell cannot build up over time. In general, chlor-alkali plants that do not recirculate brine routinely report 2–3 ppm $NaClO_3$. Plants that do recirculate

Table 4. Membranes

Membrane	Composition (Cathode ↔ Anode)	Notes
Nafion® A	2-1050CR/4-1080XR/fabric/2-1080XR	Thick membrane, PFA fibers
Nafion® B	ZrO_2/1.5-1050CR/4-1080XR/fabric/1-1080XR	Coated Nafion® E, PTFE/Dacron® sacrificial fibers
Nafion® C	ZrO_2/1-1050CR/4-1080XR/fabric/1-1080XR	Coated, Gortex®/Dacron® sacrificial fibers
Nafion® D	ZrO_2/1.5-1050CR/4-1080XR/fabric/1-1080XR/ZrO_2	PTFE fibers
Nafion® E	1.5-1050CR/4-1080XR/fabric/1-1080XR	PTFE/Dacron® sacrificial fibers
Nafion® F	ZrO_2/1-1050CR/4-1080XR/fabric/1-1080XR/ZrO_2	Roughened unhydrolysed, coated Gortex®/Dacron® sacrificial fibers
Nafion® FC	ZrO_2/1-1050CR/4-1080XR/fabric/1-1080XR/ZrO_2	Unroughened, Gortex®/Dacron® sacrificial fibers
Nafion® G	1.5-1050CR/4-1080XR/fabric/1-1080XR	Roughened, PTFE/Dacron® sacrificial fibers
Flemion 865	SiC_4/2-800'CR'/4-700'CR'/fabric/1-1080XR/ZrO_2	Dacron®/PTFE sacrificial fibers
Aciplex 11011	1-1000'CR'/4-1050'XR'/fabric/1-1050'XR'	PTFE fibers
Aciplex 41011	1-1000'CR'/4-1050'XR'/fabric/1-1050'XR'	PTFE fibers
Dow	~1-790'CR'/~3-835'XR'	No fibers

brine show much higher chlorate levels, as shown in Table 1. Thus, in a single pass process (no recycle), all membranes except the Dow membrane behave very similar in the unspiked case, and the chlorate concentrations are maintained at small values. The data show that without brine recirculation (no spiking), virtually any well-run cell could be operated with low chlorate concentrations.

By spiking the brine with 5 g l^{-1} $NaClO_3$, a simplified recycle plant cell was simulated. The resulting $NaClO_3$ in NaOH from the membranes is presented in Figure 2. The magnitude and range of the data dramatically increased to 15 to 105 ppm, the Aciplex and Flemion membranes now displaying clearly lower chlorate levels and more narrow limits of variability. In addition, membranes with and without sacrificial fibers show no evident correlation to the chlorate concentrations.

Upon comparing Figures 1 and 2, the Flemion and Aciplex membranes always yield lower chlorate concentrations, and the Dow membrane always yields the largest concentrations. This result does not seem to depend on the presence or absence of sacrificial fibers but more so on the polymer and membrane structures. The chlorate transport may be explained by a competitive mechanism involving diffusion driving the chlorates towards the cathode and migration driving the chlorates back towards the anode irrespective of the transport 'channel' size.

The Dow membrane has a lower equivalent weight (EW) than the other polymers (although an exact comparison can be made only after accounting for the differences in the side chain molecular structures). A lower EW implies a larger cation transport rate and a larger anion (chlorate) repulsion. The opposite trend is observed since the Dow membrane transports chlorates more so than the other membranes. The Dow membrane contains no fabric reinforcement which may allow excessive swelling of the membrane from electroosmosis allowing a larger chlorate transport. This membrane is somewhat thinner than the other membranes possibly allowing for a shorter chlorate diffusion path length.

For the Nafion® samples, the equivalent weights of the CR and XR polymers were kept constant. The influence of the CR layer thickness is discussed in a later section in the present paper. The presence of the surface coating ZrO_2 does not seem to measurably affect the chlorate transport as evidenced by comparing Nafion® D (coated) and E (uncoated); Nafion® E is better in the unspiked case whereas Nafion® D is better in the spiked

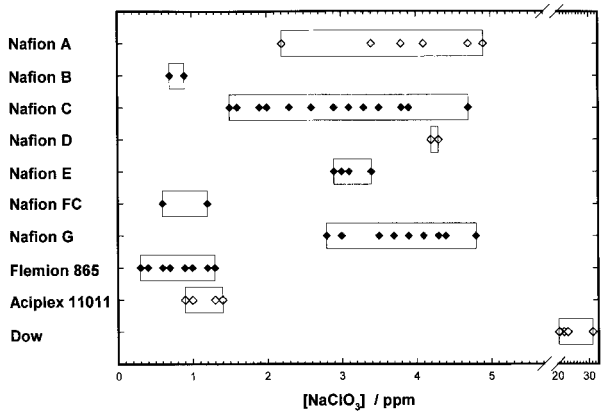

Fig. 1. Outlet chlorate concentrations for various membranes. Open symbols represent membranes with no sacrificial fibers; filled symbols are membranes containing sacrificial fibers. Cell conditions: 90 °C, 3.1 kA m^{-2}, unspiked brine.

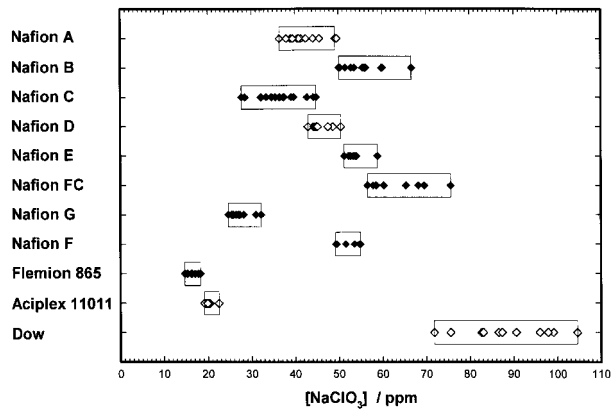

Fig. 2. Outlet chlorate concentrations for various membranes. Open symbols represent membranes with no sacrificial fibers; filled symbols are membranes containing sacrificial fibers. Cell conditions: 90 °C, 3.1 kA m^{-2}, 5 g l^{-1} chlorate spiked brine.

case yet both are fairly close together as compared to the other membranes.

The Flemion and Aciplex membranes display the lowest chlorate concentrations. Flemion is coated and contains sacrificial and PTFE fibers while Aciplex is uncoated and only contains PTFE fibers. The Aciplex membrane structure is similar (although thinner) to the Nafion® A structure. Since the thinner Aciplex structure yields lower chlorates, the chlorate diffusion path length is not the controlling variable for this case. Flemion has a very thick CR layer which may account for the large anion rejection; Aciplex, though, has a thin CR layer. The carboxylate Flemion polymer has a single ether, short side chain compared to the double ether, longer side chains of Nafion® and Aciplex. These observations imply that the very different polymer compositions influence the chlorate transport more so than small differences in the membrane construction.

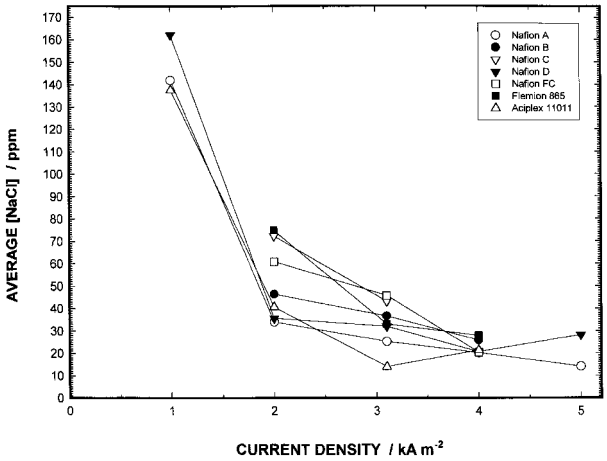

Fig. 4. Influence of the applied current density on the chloride concentration in the outlet NaOH stream for various membranes. Cell conditions: 90 °C, 5 g l^{-1} chlorate spiked brine.

3.2. *Current density*

The influence of current density on the average $NaClO_3$ and NaCl concentrations in the outlet caustic are shown in Figures 3 and 4 for a variety of ion-exchange membranes. The [$NaClO_3$] is defined as the average of all data taken under set conditions excluding startup transitions; the values thus approximate the steady-state $NaClO_3$ concentration in the caustic. Except for the 3.1 kA m^{-2} data, the [$NaClO_3$] for the Dow membrane was too high to measure with the current experimental apparatus. Each data point represents 3–5 weeks of data collection.

As a general observation, as the current density increases, both the ClO_3^- and Cl^- concentrations in the outlet NaOH decrease. This observation seems reasonable since in a chlor-alkali cell, these anions diffuse toward the cathode but migrate back toward the anode. For a given ClO_3^- spiking level in the feed brine, the diffusive flux is constant so that increasing the current density increases the back migration flux, and less ClO_3^- is transported to the NaOH side (unless the chlorate travels as a neutral species). For the Cl^- data trends, the [NaCl] in the NaOH also decreases with increasing current density because of the enhanced migration contribution to the mass transfer flux. No significant difference exists between chloride data measured in spiked or unspiked systems.

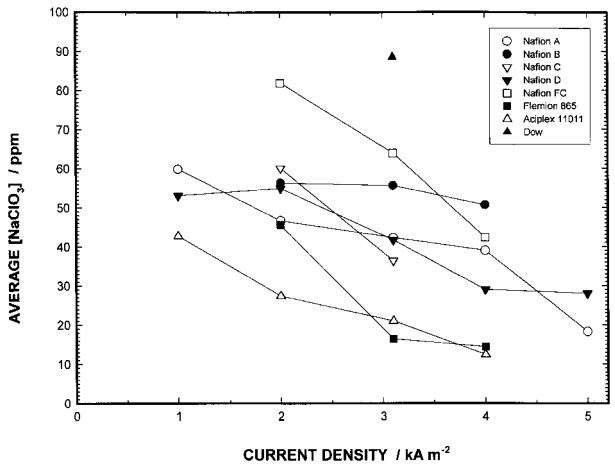

Fig. 3. Influence of the applied current density on the chlorate concentration in the outlet NaOH stream for various membranes. Cell conditions: 90 °C, 5 g l^{-1} chlorate spiked brine.

All the curves in Figures 3 and 4 are similar in slope (except for the 1 kA m^{-2} Cl^- data) which implies that the electrical migration of both anions takes place via a similar mechanism or pathway. One might expect that ClO_3^-, being a larger, more bulky anion than Cl^-, would tend to travel more sluggishly through the membrane but that does not seem to be the case at least when migration controls the mass transport. In addition, since the $NaClO_3$ in the outlet NaOH is dependent on current density, at least some of the chlorate is transported in the ionic form.

Throughout all the data, no significant influence of sulfonate membrane thickness, coatings, or fiber content is observed. The chlorate transport depends only on the polymer structure and morphology and not on the bulk membrane physical characteristics.

3.3. *Temperature*

The influence of temperature on the $NaClO_3$ and NaCl concentrations was studied although the dependence on temperature is unclear from the data obtained. The $NaClO_3$ concentration, however, did increase slightly with temperature. If migration and diffusion are the competing modes of transport, both the conductivity and diffusion coefficient depend on temperature. Since the chlorate concentration gradually increases at higher temperatures, the diffusion coefficient must be increasing at a faster rate than the conductivity since the fluxes are in opposite directions. Also, the slope of the concentration dependence on temperature is fairly constant yet the intercepts of these curves varied among the membranes tested.

3.4. *Carboxylate film thickness*

As is well known, a carboxylate salt film acts to reject and hinder transport of anions through the membrane. The film is not as ionically conductive as the sulfonate polymer so in most commercial membranes, the sulfonate and carboxylate structures are bonded together to obtain the best properties of both films. In general, a thicker carboxylate layer has been observed to raise the current efficiency, but unfortunately, the cell voltage also increases. Anionic transport, however, is a very complex phenomenon owing to competition between the migration, diffusion and convective modes of mass transfer. A theoretical and experimental approach is taken to study the effect of the carboxylate film thickness on chlorate transport. The resulting analysis is general enough to apply to other ions as well as chlorates.

An ion is transported through an ion-exchange membrane by three different mechanisms which may act in the same or opposite directions. The ion may diffuse through the membrane if there exists a concentration gradient between the cathode and anode sides of the membrane. The ion may also migrate through the membrane if an electric field is set up across the membrane thereby establishing a potential gradient. Another mode of mass transfer, convection, takes place in the membrane due to an electroosmotic force within the membrane channels. The diffusion and convection transport act in the same direction and opposite to the migration transport. Conceivably, one could imagine cases where one mode may dominate the overall transport (diffusion dominates at high chlorate concentrations in the anolyte while migration dominates at high current density).

To model the chlorate transport through a membrane, the total mass transfer of species i is evaluated as the summation of the migration, diffusion and electroosmotic convection fluxes, as given by Equation 1.

$$N_i = -z_i \mu_i F C_i \nabla \phi + D_i \nabla C_i + v C_i \tag{1}$$

where, N_i = total molar flux of species i (mol cm^{-2} s^{-1}), z_i = electronic charge number of species i, μ_i = mobility of species i (cm^2 mol J^{-1} s^{-1}), F = faradaic constant (96 484.6 C equiv^{-1}), C_i = concentration of species i (mol cm^{-3}), ϕ = electrical potential (V), D_i = diffusion coefficient of species i (cm^2 s^{-1}), and v = electroosmotic flow velocity (cm s^{-1}). Note that in Equation 1, all gradients (∇) are positive.

Considering the mass transfer only in one direction (x, through the membrane), Equation 1 simplifies to

$$N = -z\mu F C \frac{\partial \phi}{\partial x} + D \frac{\partial C}{\partial x} + vC \tag{2}$$

where the subscript i is omitted since only the chlorate ion is considered.

The ratio of the chlorate flux through a thin carboxylate layer to the flux through a thick carboxylate layer is given by

$$\frac{N_{\text{thin}}}{N_{\text{thick}}} = \frac{\left(D\frac{\partial C}{\partial x} + vC - z\mu F C \frac{\partial \phi}{\partial x}\right)_{\text{thin}}}{\left(D\frac{\partial C}{\partial x} + vC - z\mu F C \frac{\partial \phi}{\partial x}\right)_{\text{thick}}} \tag{3}$$

The partial derivatives are approximated by linear terms realizing that this simplification is not valid for the concentration profile. The physical meaning, however, will be clearer and the conclusions will remain the same.

$$\frac{N_{\text{thin}}}{N_{\text{thick}}} = \frac{D\frac{\Delta C}{L} + vC - z\mu F C \frac{\Delta \phi_{\text{thin}}}{L}}{D\frac{\Delta C}{L+T} + vC - z\mu F C \frac{\Delta \phi_{\text{thick}}}{L+T}} \tag{4}$$

L is the thickness of a thin membrane and T is an added thickness so that $L + T$ is the thickness of a thick membrane.

The potential gradient is constant irrespective of the film thickness, as given by Equation 5.

$$\frac{\Delta \phi_{\text{thin}}}{L} = \frac{\Delta \phi_{\text{thick}}}{L+T} \tag{5}$$

This assumption is valid for all the constant current experiments performed in the present paper. Therefore, in cases where migration dominates chlorate mass transfer, the thickness of the carboxylate layer does not affect the chlorate transport.

As the membrane becomes thicker ($L + T$ increases), $\Delta C/(L + T)$ decreases, and Equation 4 becomes

$$\frac{N_{\text{thin}}}{N_{\text{thick}}} > 1 \tag{6}$$

Therefore, the thicker the membrane, the smaller the ClO_3^- flux when diffusion is the dominant mode of chlorate mass transfer.

For a thicker film, the potential difference ($\Delta\phi$) increases but so does the thickness so the migration driving force (the potential gradient, $\Delta\phi/\Delta x$) is constant. However, for a thicker film, the concentration difference (ΔC) between the two sides of the film is a constant but the thickness increases; therefore, the diffusion driving force ($\Delta C/\Delta x$) decreases and less ClO_3^- is transported toward the cathode.

A mass balance for the transport of the chlorate ions is given by [27]

$$\frac{\partial C_i}{\partial t} = -\nabla \cdot N_i + R_i \tag{7}$$

where t is time (s) and R_i is the bulk reaction rate (mol s^{-1} cm^{-3}). For the special case of one-dimensional transport, a constant potential gradient, steady state, and no bulk reaction, the solution for Equations 1 and 7 is given by

$$C = C_c + \left(\frac{C_a - C_c}{e^{-\frac{a}{D}L} - 1}\right)\left(e^{-\frac{a}{D}x} - 1\right) \quad (8)$$

where a (in cm s^{-1}) is a parameter given by

$$a = v - zF\mu\left(\frac{\partial\phi}{\partial x}\right) = v - \frac{zFD}{RT}\left(\frac{\partial\phi}{\partial x}\right)$$

$$a \approx v - \frac{zFD}{RT}\left(\frac{\Delta\phi}{L}\right) \quad (9)$$

where C_c = catholyte concentration (ppm) and C_a = anolyte concentration (ppm). Equation 9 was obtained with use of the Nernst–Einstein relation.

Equation 8 was used to compute the chlorate concentration profile through the membrane, as shown in Figure 5. Both the temperature and voltage were used as parameters, and the electroosmotic flow velocity was taken to be zero. The model shows that temperature has a small effect on the profile while changing the potential has a relatively large effect. For a 6 mil thick membrane, virtually the entire concentration change occurs over 2 mil on the anode side.

The electroosmotic velocity is now varied to observe the effect of the velocity on the concentration profile, as shown in Figure 6. The model is very sensitive to small changes in the flow velocity. To approximate the actual flow velocity, Equation 6 in [11] was used. For the computation, the actual measured values from the laboratory cells were used instead of the empirical correlations listed in [11]. For a current density of 3.1 kA m^{-2} and a caustic current efficiency of 95%, the velocity was computed to be 2.5×10^{-4} cm s^{-1}. This value will vary depending on the cell operating conditions. The electroosmotic flow adds to the diffusional flux to promote chlorate transport so by minimizing the convective flow the chlorate transport will decrease.

To test the theoretical ideas presented above, a number of Nafion® membranes of different carboxylate film thicknesses were examined at 3.1 kA m^{-2} and 90 °C. The [$NaClO_3$] was measured in the exit catholyte stream as the anolyte was spiked at $NaClO_3$ concentrations from 0 to 20 g l^{-1}. The results are presented in Figure 7. Note that other variables besides the carboxylate film thickness could not be kept constant with these commercial membranes, but the results presented in the previous sections suggest that these other variables (surface coating, sacrificial fibers, etc.) do not play a significant role in chlorate transport.

The experimental results reflect the theoretical ideas rather well. At very high spiking levels (10 and 20 g l^{-1} $NaClO_3$), the diffusion of the chlorate overwhelms the migration flux so that a thicker carboxylate film simply represents a larger diffusion path. Less chlorate is thus transported in thicker membranes. At 5 g l^{-1} or less, the migration and diffusion fluxes are similar so the carboxylate layer thickness has little or no influence on the chlorate transport.

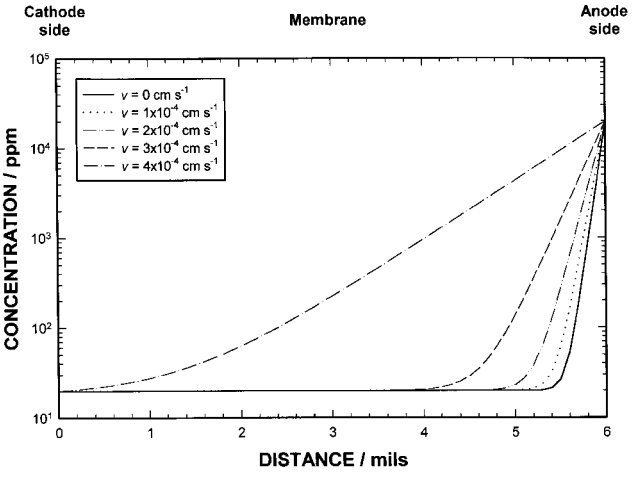

Fig. 6. Effect of electroosmotic flow on the theoretical concentration profiles through a 6 mil ion-exchange membrane for 5 g l^{-1} chlorate spiked brine; T = 90 °C and ϕ = 3 V.

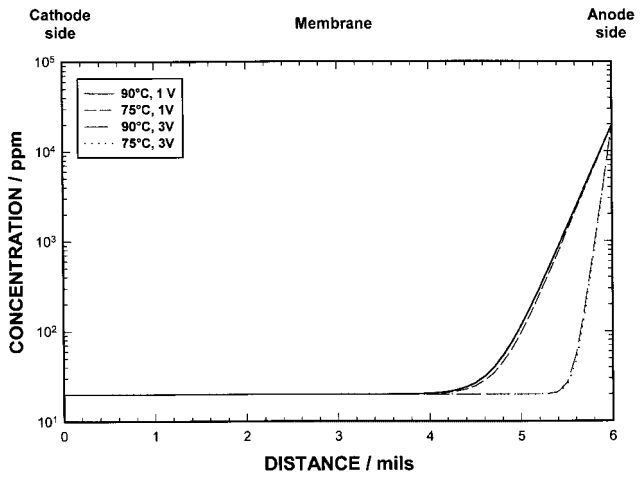

Fig. 5. Effects of temperature and voltage on the theoretical concentration profiles through a 6 mil ion-exchange membrane for 5 g l^{-1} chlorate spiked brine; $v = 0$ cm s^{-1}.

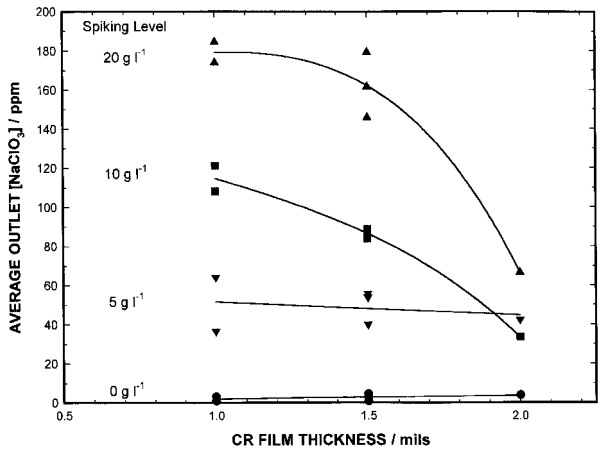

Fig. 7. Experimental chlorate concentration measurements in the outlet NaOH stream at various anolyte chlorate spiking levels as a function of the carboxylate film thickness. Cell conditions: 3.1 kA m^{-2}, 90 °C.

Variables, such as the diffusion coefficient and the mobility of chlorate ions, are needed before quantitative comparisons can be drawn between the theoretical and experimental results. The trends, however, are clear. The carboxylate film thickness only affects the chlorate transport above a critical anolyte chlorate concentration (5 g l^{-1}) at a constant current density. Furthermore, if the current density (or potential) is increased (thereby increasing the migration flux back toward the anode), the critical chlorate concentration should increase; that is, more than 5 g l^{-1} $NaClO_3$ would have to be added to the anolyte for the carboxylate film thickness to influence the chlorate transport.

3.5. *Brine spiking*

The amount of chlorate in the anolyte brine is expected to have a profound effect on the chlorate in the catholyte stream if diffusion is a main mode of transport. To examine this phenomenon, several ion-exchange membranes were evaluated in laboratory cells while the anolyte was spiked with 0 to 20 g l^{-1} $NaClO_3$. The cell was operated galvanostatically at 3.1 kA m^{-2} and isothermally at 90 °C. The chlorate levels were taken over a period of weeks as a function of the inlet brine concentration, and the steady state values are presented in Figure 8.

Figure 8 shows as the chlorate level in the brine is increased, so is the chlorate concentration in the caustic. The empirical relationships obtained from Figure 8, where C_{in} is the anolyte input chlorate concentration (g l^{-1}) and C_{out} is the outlet catholyte chlorate concentration (ppm), are

$$\begin{aligned} &\text{Flemion:} && C_{out} = 2.4\,C_{in} \\ &\text{Aciplex:} && C_{out} = 2.9\,C_{in} \\ &\text{Nafion®:} && C_{out} = (6 \text{ to } 9)\,C_{in} \\ &\text{Dow:} && C_{out} = 13\,C_{in} \end{aligned} \qquad (10)$$

indicating that Flemion rejects chlorates the best of all membranes tested. Changes in the physical and chemical form of the membranes lead to large differences in the magnitude and slope of these systems depending on the polymer structure. Such a difference in these slopes indicates that the ionic transport is greatly altered by adjusting the polymer properties.

4. Conclusions

Data are presented to obtain an understanding of the transport of chlorate ions in chlor-alkali membrane cells. The long term goal is to develop a membrane which, when placed in an operating cell, produces less than 10 ppm $NaClO_3$ in the NaOH product. Data taken on Nafion®, Flemion, Dow and Aciplex membranes show that much lower chlorate concentrations are present using the Flemion and Aciplex membranes in a spiked brine (recycle) system, but all membranes are comparable in an unspiked (single pass) process. In addition, the presence or absence of sacrificial fibers does not seem to correlate strongly to the resultant chlorate concentrations.

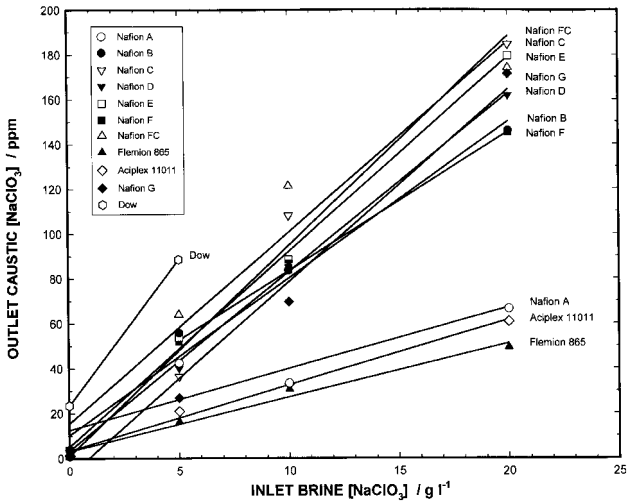

Fig. 8. Effect of chlorate spiking of the anolyte input stream for various membranes. Cell conditions: 3.1 kA m^{-2}, 90 °C.

Basic cell data show that sulfonate film thickness, surface coatings and fiber content had no influence on the chlorate transport. Increasing the current density in a cell increases the migration flux of chlorate back toward the anode inhibiting transport to the cathode compartment. Temperature has very little influence on chloride transport but increases chlorate transport presumably by increasing the chlorate diffusion coefficient. The structure of the membrane has a minor influence on chlorate transport; the basic polymer structure and morphology are the main variables which control the transport.

Commercial Nafion® membranes of varying carboxylate film thicknesses (from 1 to 2 mil) were tested to examine the relationship between carboxylate film thickness and chlorate transport. A critical chlorate anolyte concentration of 5 g l^{-1} $NaClO_3$ at 3.1 kA m^{-2} and 90 °C was observed where the chlorate migration and diffusion fluxes are comparable. Above this critical concentration, diffusion dominates the transport, and a thicker carboxylate layer yields a smaller chlorate concentration in the catholyte. Below this critical concentration, migration dominates diffusion and the carboxylate film thickness has no influence on the chlorate transport.

As commercial chlor-alkali producers continue to increase their current densities in operating cells, the chlorate concentration in the NaOH will continue to decrease. At current densities of 5 kA m^{-2} or higher, most of the membranes will produce NaOH with less than 10 ppm $NaClO_3$. One would expect that at lower spiking levels, the ClO_3^- against current density slope should increase as the migration flux becomes more comparable to the diffusion flux. As the spiking level increases, the diffusion should become more of an influence and the slope should decrease.

Another consideration is that chemical producers strive to attain closed loop process control so brine recirculation will become necessary. Although better control of the process may be attained, the continuous buildup of chlorate in the anolyte stream will produce a more impure NaOH product. A balance must be achieved between the operating conditions and the process design to minimize the resultant chlorate concentration.

Acknowledgements

Our most sincere gratitude to Dr J.T. Keating (DuPont) for discussions on this topic and to T. Norton, Gr. McCauley, D. Gedling and H. Moore for testing the membranes.

References

1. D.J. Pye, *US Patent 2 610 105* (1952).
2. C.C. Brumbaugh, *US Patent 2 562 169* (1951).
3. NACE Task Group T-5A-9C, Final Report, Materials Protection and Performance Publication 5A271 (1971), p. 39.
4. S.M. Reddy, J.W. Norris and S.A. Perusich, *J. Appl. Electrochem.* in preparation.
5. F. Foerster and E. Muller, *Z. Elektrochem.* **8** (1902) 515.
6. N. Ibl and D. Landolt, *J. Electrochem. Soc.* **115** (1968) 713.
7. D. Landolt and N. Ibl, *Electrochim. Acta* **15** (1970) 1165.
8. A. Tasaka and T. Tojo, *J. Electrochem. Soc.* **132** (1985) 1855.
9. L. Hammar and G. Wranglen, *Electrochim. Acta* **9** (1964) 1.
10. F. Hine and M. Yasuda, *J. Electrochem. Soc.* **118** (1971) 182.
11. C.-P. Chen and B.V. Tilak, *J. Appl. Electrochem.* **26** (1996) 235.
12. L.L. Benezra, D.W. Hill, A. Riihimaki and T. Shan-Pu, *US Patent 4 055 476* (1977).
13. *British Patent 506 394* (1939).
14. S.G. Osborne and A. Mitchell, *US Patent 2 569 329* (1951).
15. G.E. Galecki and S.R. Oberson, *US Patent 3 891 747* (1975).
16. P. Lai, S. Szymanski and N.L. Christensen, *US Patent 4 169 773* (1979).
17. W.A. McRae, *US Patent 4 230 544* (1980).
18. S.H. Moore and R.L. Dotson, *US Patent 4 405 465* (1983).
19. S.H. Moore and R.L. Dotson, *US Patent 4 481 088* (1984).
20. Y. Samejima, M. Shiga, T. Kano and T. Kishi, *US Patent 4 643 808* (1987).
21. I.E. Muskat, *US Patent 2 207 595* (1940).
22. A.K. Johnson, *US Patent 2 790 707* (1957).
23. D.L. Fair, D.D. Justice and K.E. Woodard, *US Patent 4 528 077* (1985).
24. A. Sakata and K. Suzuki, *Jpn Patent 86-272 985* (1988).
25. S.A. Perusich, *Macromolecules* **33** (2000) 3437.
26. L.L. Stookey, *Anal. Chem.* **42** (1970) 779.
27. J.S. Newman, 'Electrochemical Systems', 2nd edn (Prentice Hall, Englewood Cliffs, NJ, 1991).